

A Prototype AMSR-E Global Snow Area and Snow Depth Algorithm

Richard E. Kelly, Alfred T. Chang, *Fellow, IEEE*, Leung Tsang, *Fellow, IEEE*, and James L. Foster

Abstract—A methodologically simple approach to estimate snow depth from spaceborne microwave instruments is described. The scattering signal observed in multifrequency passive microwave data is used to detect snow cover. Wet snow, frozen ground, precipitation, and other anomalous scattering signals are screened using established methods. The results from two different approaches (a simple time and continentwide static approach and a space and time dynamic approach) to estimating snow depth were compared. The static approach, based on radiative transfer calculations, assumes a temporally constant grain size and density. The dynamic approach assumes that snowpack properties are spatially and temporally dynamic and requires two simple empirical models of density and snowpack grain radius evolution, plus a dense media radiative transfer model based on the quasicrystalline approximation and sticky particle theory. To test the approaches, a four-year record of daily snow depth measurements at 71 meteorological stations plus passive microwave data from the Special Sensor Microwave Imager, land cover data and a digital elevation model were used. In addition, testing was performed for a global dataset of over 1000 World Meteorological Organization meteorological stations recording snow depth during the 2000–2001 winter season. When compared with the snow depth data, the new algorithm had an average error of 23 cm for the one-year dataset and 21 cm for the four-year dataset (131% and 94% relative error, respectively). More importantly, the dynamic algorithm tended to underestimate the snow depth less than the static algorithm. This approach will be developed further and implemented for use with the Advanced Microwave Scanning Radiometer—Earth Observing System aboard Aqua.

Index Terms—Dense media radiative transfer model, microwave radiometry, remote sensing, snow depth.

I. INTRODUCTION

SNOW COVER estimation is important for climate change studies and successful water resource management. It has been shown that snow cover can affect directly climate dynamics [1], and so our ability to estimate global snow coverage and volumetric storage of water in seasonal and permanent snowpacks impacts on our ability to monitor climate and climate change and to test climate model simulations.

Manuscript received April 30, 2002; revised December 20, 2002. This work was supported by the National Aeronautics and Space Administration Office of Earth Sciences Program and by the EOS AMSR-E Algorithm Development Project.

R. E. Kelly is with the Goddard Earth Science and Technology Center, University of Maryland—Baltimore County, Baltimore, MD 21250 USA (e-mail: rkelly@glacier.gsfc.nasa.gov).

A. T. Chang and J. L. Foster are with the Hydrological Sciences Branch, NASA Goddard Space Flight Center, Greenbelt, MD 20771 USA (e-mail: Alfred.T.Chang@nasa.gov; James.L.Foster@nasa.gov).

L. Tsang is with the Department of Electrical Engineering, University of Washington, Seattle, WA 98195 USA (e-mail: tsang@ee.washington.edu).

Digital Object Identifier 10.1109/TGRS.2003.809118

Furthermore, successful estimation of volumetric storage of snow water at a basin scale should improve the management of water supply. Remote sensing has been used to monitor continental scale seasonal snow covers for 25 years [2] with much of this effort focused on the use of remote sensing of snow cover area using visible and infrared sensors [3], [4]. While this effort is starting to mature, the successful estimation of global snow volume [snow depth or snow water equivalent (SWE)] is still at a developmental stage.

Progress in retrieving snow depth or SWE has been made through the available “instruments of opportunity” such as the Scanning Multichannel Microwave Radiometer (SMMR) and the Special Sensor Microwave Imager (SSM/I). Neither instruments were designed explicitly for snow applications but have been found to be effective for this application [5], [6]. For snow detection, passive microwave instruments tend to underestimate the snow area compared with estimates from visible-infrared snow mapping methods [7]. Additionally, the errors of estimates of snow volume tend to be large with standard errors of 20 mm SWE and greater not uncommon (e.g., see [8]). The perceived need by water resource managers and land surface and climate modelers is for high accuracy, local scale estimates of snow volume on a daily basis. Unfortunately, the spatial resolution of the SMMR and SSM/I instruments tends to restrict their effective use to regional-scale studies. Furthermore, currently available SSM/I data is acquired twice daily only at high latitudes with coverage more restrictive at lower latitudes. The Advanced Microwave Scanning Radiometer—Earth Observing System (AMSR-E) aboard Aqua, which was launched in 2002, should help to overcome some of these drawbacks. Table I gives selected details of the AMSR-E and SSM/I configurations and while AMSR-E temporal coverage is similar, its spatial the resolution is generally finer than that of the SSM/I. Overall, technological improvements should be matched by the improvements in snow cover estimation. However, there is a need to develop a global snow monitoring algorithm (area and volume) that is temporally and spatially dynamic so that current retrieval errors can be reduced further.

This paper describes the development and testing of an algorithm to estimate global snow cover volume from spaceborne passive microwave remote sensing observations. Our aim is to detect snow cover area globally and then to estimate the snow depth for the snow area. The microwave brightness temperature emitted from a snow cover is related to the snow mass which can be represented by the combined snow density and depth, or the SWE (a hydrological quantity that is obtained from the product of snow depth and density). Two issues emerge from this relationship that require some consideration. The first is theoretical

TABLE I
COMPARISON OF AQUA AMSR-E [9] AND SSM/I SENSOR CHARACTERISTICS [10]

AMSR-E	Center Freq (GHz)	6.9	10.7	18.7	23.8	36.5	89.0
	Band Width (MHz)	350	100	200	400	1000	3000
	Sensitivity (K)	0.3	0.6	0.6	0.6	0.6	1.1
	IFOV (km x km)	76 x 44	49 x 28	28 x 16	31 x 18	14 x 8	6 x 4
SSM/I	Center Freq (GHz)			19.35	22.235	37.0	85.5
	Band Width (MHz)			240	240	900	1400
	Sensitivity (K)			0.8	0.8	0.6	1.1
	IFOV (km x km)			69 x 43	60 x 40	37 x 29	15 x 13

in nature and the second is of a practical consideration. First, in regions where SWE data are sufficiently available, microwave algorithms have been developed to estimate SWE (e.g., [8] and [11]). To estimate snow depth alone using passive microwave observations, assumptions about the snow density need to be made because microwave radiation is sensitive to both depth and density and not just one variable alone. This is the reason why previous “static” algorithms have worked reasonably well for average seasonal and global snow depth estimation. At the local scale, however, and over short time periods, estimates have been subject to errors as a result of rapid changes in internal snowpack properties (density, layering) to which the microwave response is sensitive. Thus, the implication is that algorithms should be developed to estimate not snow depth but SWE which is a bulk property of the snowpack that directly influences the microwave response. Second, however, and counter to the first issue, is that on a practical level and for the validation of a global algorithm there are consistently and considerably fewer global SWE measurement sites than there are snow depth measurement sites. One could develop a SWE algorithm but there are so few data globally available with which to test the estimates so that traditional validation would be a problem. In this paper, therefore, in the absence of global SWE validation datasets, our effort is concerned on a practical level with snow depth estimation, which has a greater global validation potential.

II. BACKGROUND

In this paper, we use the difference between low (19 GHz) and high (37 or 85 GHz) frequency brightness temperatures from the SSM/I to detect scattering sources; a positive difference is regarded as a scatterer and might possibly have been emitted by the snow [12]. Generally, the greater this difference, and hence, the scattering signal, the greater the snow volume assumed to be present. Unfortunately, a major problem with this assumption is that in nature, changes to snowpack physical properties can also cause changes to the microwave scattering response of the pack; a change in the observed scattering equally might be caused by an increased snow volume or a change in the physical structure of the snow resulting from snowpack metamorphism. For homogeneous snowpacks, the scattering signal can be converted to SWE or snow depth using an empirical algorithm or physically based static algorithm. This approach is often static in character in the sense that constant “average” snow conditions (grain size, density) are used to parameterize the algorithm for application globally and throughout the entire winter season. Some success has been achieved from this methodology (e.g., see [5], [11],

[13], and [14]), and as Armstrong *et al.* [15] notes, the success of these algorithms might be because the mean grain size variations over passive microwave footprints are not substantial. When snowpack physical properties are heterogeneous in both horizontal and vertical space and through time (as is often the case in nature), deterministic models of electromagnetic radiation emission from the snow coupled with a hydrological model of the snowpack have been successful in estimating snow depth [6]. However, the drawback at the global scale for the more complex physically based modeling approach is that it is often site specific or requires snowpack parameterization from *in situ* observations. Furthermore, implementation is achieved using multiple high quality input snowpack parameters that are often not available globally; Armstrong *et al.* [15] concludes that detailed numerical description of the snow structure within a passive microwave footprint probably is neither possible nor practical to obtain. Therefore, an alternative, nonsite specific strategy of parameterizing the pack is desirable that is more generic but which can be used to describe the space and time varying average state of the local pack.

The naturally emitted microwave brightness temperature (T_b) of a snowpack is related to several components. Primarily, the number of snow grains along the emission path (the snow depth in centimeters), the size of grains (grain radius in millimeters), and the packing of the grains (volume fraction in percentage or density in kilograms per cubic meter) are probably the most important factors controlling the propagation of radiation at higher frequencies (e.g., 37 GHz). Snow physical temperature also affects snow emissivity [16], although it is considered of secondary importance compared with grain size, density and snow depth. Furthermore, by using a brightness temperature difference between 19 and 37 GHz ($T_{b19}-T_{b37}$), the snow temperature effect is minimized.

Beneath the snowpack, the subnivean soil roughness and dielectric properties can be important for emitted microwave radiation. Hoekstra and Delaney [17] showed that at temperatures less than 0 °C, when the soil is frozen, the imaginary part of the dielectric constant of soil is invariant for any given water content up to 15%. The real part of the soil dielectric constant is slightly different for different moisture contents but does not change appreciably with temperature. Hallikainen *et al.* [18] found that for different frozen soils, these dielectric properties are constant between 19 and 37 GHz. Thus, by using the $T_{b19}-T_{b37}$ difference, the effect of the dielectric properties on the brightness temperature difference is effectively canceled out. For soil temperatures greater than 0 °C, if the soil is dry, the dielectric constant behaves the same as its frozen state. If the soil is wet, frequency

dependent changes to the dielectric constant can be observed and will affect upwelling radiation through and from the snow.

With respect to the surface roughness of a dry soil, Schmugge [19] demonstrated that its effect on microwave emission is small. Hence, by using a brightness temperature difference factor, this effect is almost completely removed from the retrieval process. If the soil is wet, the soil roughness exerts a greater influence on the upwelling emission. Overall, the largest impact on snowpacks from roughness and dielectric properties are most likely to be located in maritime regions where soil temperatures are above freezing particularly when the soil is wet. In other parts of the world that are dominated by seasonal continental snowpacks, soil temperatures are at or below freezing, and the soil roughness and dielectric properties can probably be disregarded.

For this paper, therefore, we assume that the soil temperature at the base of a snowpack is less than or equal to 0 °C so that the dielectric constant and soil surface roughness are assumed to have a negligible effect on the microwave emission from the snow. We assume that average snow grain radius, density, and depth are the prime controls of microwave emission from the snow and that the snow temperature is of secondary importance to these three variables. We then implement two conceptually simple models of average bulk grain size and average bulk snow density that can be varied in space and time using estimated surface kinetic temperature information. While lacking complexity of more comprehensive snowpack models, our approach has the advantage that it can be applied easily at a global scale. The method is not time independent; it is assumed that the snowpack grain size and density have histories and so the method cannot be implemented successfully without prior knowledge of the pack evolution. Once the grain size and density have been estimated at a given time step, a dense media radiative transfer (DMRT) model based on the quasi-crystalline approximation (QCA) and sticky particle theory is used to estimate the snow depth together with observed SSM/I data.

III. DATASETS USED AND GEOGRAPHICAL PARAMETERS

For global studies, it is impossible to obtain a comprehensive and internally consistent set of SWE measurements for any given winter season since generally they do not exist except in a few local regions around the world. Therefore, the methodology developed here is tested using snow depth observations collected globally, albeit at various levels of quality. In the absence of spatially intensive snow depth measurements, the available extensive data are often the only globally consistent data available. Two datasets from the World Meteorological Organization (WMO) Global Telecommunications System (GTS) network were used in this paper for algorithm development and testing purposes. Hereafter the data are referred to as WMO-GTS data. First, a dataset consisting of 100 distributed Northern Hemisphere meteorological stations obtained from the WMO-GTS archive [20] was used to test the grain growth model. These early morning daily data cover the period from January 1992 to December 1995 (inclusive). They were quality controlled to remove 29 stations that contained substantially anomalous or erroneous data. Such examples were sites where

poor quality snow depth measurements were taken (no variation in snow depth from month to month), stations with close proximity to large water bodies and stations located in mountainous terrain. Fig. 1 shows the location of the 71 meteorological stations comprising the four-year record. Second, a set of daily snow depth measurements spanning October 2000 to April 2001 (inclusive) from the WMO-GTS data archive was also used.¹ 8000 stations comprise this second dataset although less than 1500 stations record snow depth with any regularity. For both datasets, snow depth measurements were converted from inches to meters and reprojected to the 25-km Equal Area Scaleable Earth Grid (EASE-grid) [21]. Also, global SSM/I swath data were acquired for each day in the two WMO-GTS records. SSM/I brightness temperature measurements were reprojected to the EASE-grid projection and for each day, the geographically closest suite of SSM/I brightness temperature samples (19-, 22-, 37-, and 85-GHz channels) were paired with spatially coincident snow depth observations.

Problems exist with the WMO-GTS data since snow depth is not the prime measured variable; snow depth records are present but sometimes only on a very irregular basis (especially during the early and late times in the winter season). Furthermore, an assumption is made that station measurements of snow depth were representative of the average 25 × 25 km EASE-grid cell snow depth. However, in many regions, terrain and vegetation are heterogeneous [22] and can produce large spatial variations in snow depth within an EASE-grid cell. Nevertheless, despite these drawbacks, the WMO data were used, as they constituted the only independent means of quantifying global snow depth on the ground. In the following sections the 1992–1995 WMO-GTS data with coincident SSM/I observations were used for both algorithm development (Section IV) and algorithm testing (Section V). The 2000–2001 WMO-GTS data and SSM/I observations were used for algorithm testing only (Section VI).

IV. ALGORITHM DEVELOPMENT

A. Snow Detection

For a global algorithm, it is important to identify only areas that might have snow present. The climatological probability of snow cover presence is obtained from [23] and [24]; if a pixel is located where the presence of snow cover is climatologically rare, this pixel is flagged as no snow. In addition, ice sheets and complex mountainous terrain are also screened from the algorithm since these terrains are dominated often by complex microwave signals for which the snow retrieval is very difficult. If a pixel is located where snow is possible, the microwave signal is tested for scattering. A surface scattering signal can be detected using the expression developed by Chang *et al.* [5] to estimate snow depth using microwave observations

$$SD = a(Tb18H - Tb36H) \text{ [cm]}. \quad (1)$$

SD is the snow depth and Tb18H and Tb36H are the horizontally polarized brightness temperatures at 18 and 36 GHz,

¹<http://wlf.ncdc.noaa.gov/> (last visited 6/11/2002)

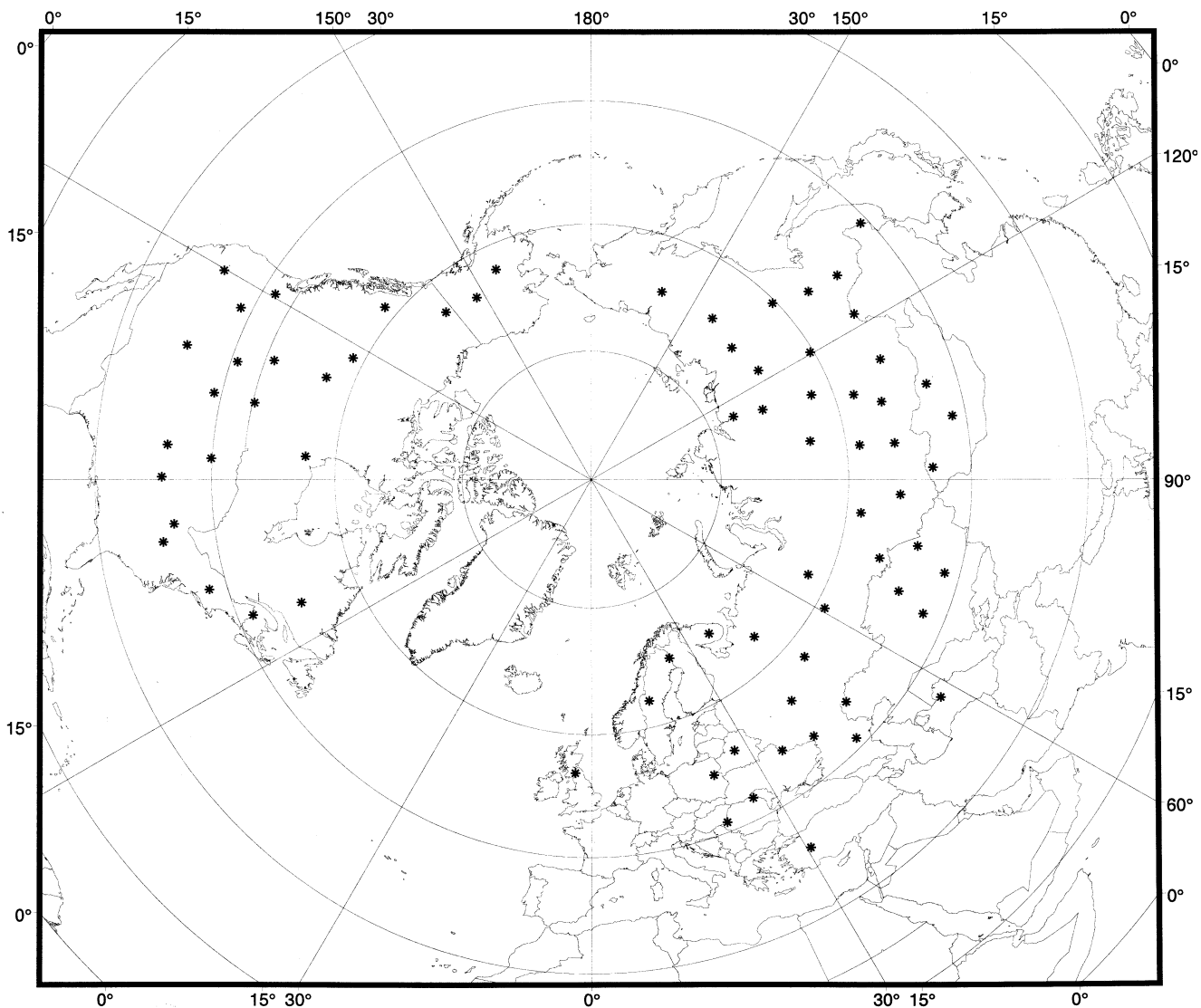


Fig. 1. Location of the 71 meteorological stations used to recalibrate the snow depth retrieval algorithm mapped to the EASE-grid projection.

respectively, and a is a coefficient (1.59 cm K^{-1}) determined from radiative transfer model experiments of snow. In that study, the grain radius and snow density was assumed to be 0.3 mm and 300 kg m^{-3} , respectively. The algorithm was developed for use with SMMR, and Armstrong and Brodzik [7] has shown that a -5-K adjustment to the $(\text{Tb}_{18\text{H}} - \text{Tb}_{37\text{H}})$ term is required when the algorithm is applied to SSM/I data (on account of differences in SSM/I channel central frequencies compared with SMMR). If SD is greater than 0 cm then the original algorithm flags the presence of snow. Confusion of surface category can occur when other nonsnow scattering surfaces are present, especially rainfall, cold desert, and frozen ground. Using the approach described in [25], these nonsnow surfaces are screened. In addition, wet snow, which has a negligible scattering signal, is excluded from the retrieval using the method in [26].

There is some question about the choice of polarization that should be used in (1). From ground-based microwave measurements, Mätzler [27] has shown that the horizontally polarized channels at 19 and 37 GHz are slightly more sensitive to snowpack stratigraphy than the vertically polarized channels. How-

ever, for spaceborne passive microwave observations over large footprints, Rango *et al.* [28] demonstrated that that Tb 's at horizontal and vertical polarization have very similar relationships with snow depth or snow water equivalent. Furthermore, when using a Tb difference algorithm at these two frequencies, the snowpack stratigraphy effects in one channel frequency will be very similar to the effects in the other. To detect snow, it could be argued that the horizontal polarization channels are more appropriate (as they are very slightly sensitive to a marginally greater range of snowpack properties) while for snow depth estimation, the vertical polarization channels are very slightly less affected by the snowpack properties.

B. Snowpack Grain Growth

During the seasonal metamorphism of a snowpack there are distinct phases which affect directly the microwave response of the snow. It has been noted that the snowpack grain size is important for the microwave behavior of the snow [29]. Generally, the snow density and grain radius is the smallest on deposition [30]. After about two to three days, the grains start to

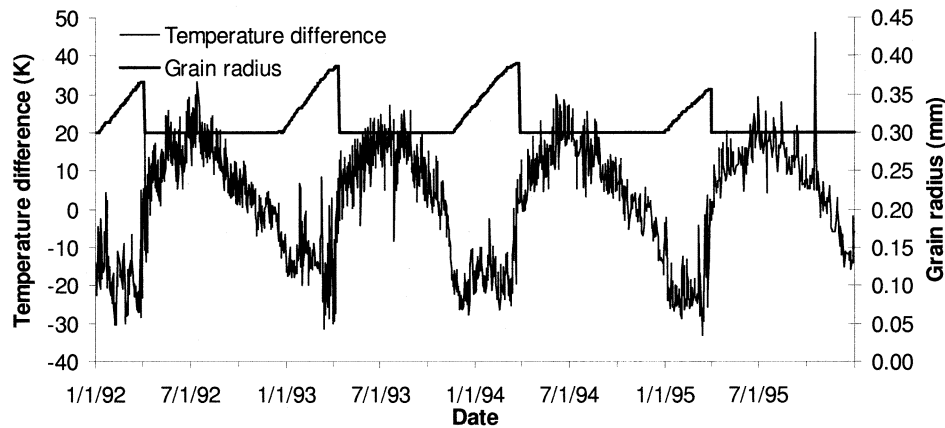


Fig. 2. Variation of grain size and temperature difference for a meteorological station in Russia ($58^{\circ} 52' 12''$ N, $78^{\circ} 21' 00''$ E) between 1992–1995 inclusive.

sinter naturally, a process whereby the crystal branches break down and snow crystals begin to become rounded and physically cohesive. Under equitemperature growth conditions (small temperature gradient through the snowpack), theoretically, this rounding can take a long time; qualitative observations in the laboratory suggest that this is a slow process that can take several weeks. It is characterized by slow grain radius growth rates and we use a constant rate of $0.0001 \text{ mm day}^{-1}$. This rate is an approximation and not rigorously tested and so requires further investigation. However, it seems slow enough to produce sub-millimetric changes to the grain size over months. Alternatively, under kinetic growth conditions where the thermal and vapor gradient is large, snow grain radii can grow rapidly; the branches break down and the snow loses its cohesive strength. Sturm and Benson [31] expressed this growth characteristic using a logistic curve for the evolution of surface and bottom snow layers. They formulated an empirical equation for radius growth where r is the radius in the form

$$r(t) = r_{\infty} - (r_{\infty} - r_0) \exp(-kt) \text{ [mm]} \quad (2)$$

where r_0 is the initial grain size; r_{∞} is the limiting grain size; k is a constant; and t is the time elapsed from the start of growth. This is a generalized form that applies to depth hoar development for grains of minimum size 0.5 mm. However, we use this relationship to approximate the general rate of change of average grain radius growth in a snowpack under kinetic growth conditions. We assume a minimum and a maximum grain radius of 0.2 and 1.0 mm, respectively, and the growth coefficient k is set to 0.01, which is the snowpack bottom growth coefficient reported in [31]. The minimum grain radius is probably too large with respect to natural snow covers. However, for microwave remote sensing, an average grain size of less than or equal to 0.1 mm would produce very little discernible interaction with passive microwave radiation rendering the snowpack invisible to the imagery. Hence, we use a larger grain radius to initialize the pack.

All three snowpack thermal phases (fresh snow, equitemperature, and kinetic temperature) can affect changes to the average snowpack grain radius characteristics, which in turn affects the microwave response from snow. The threefold classification is simplistic and may not account for complex metamorphic pro-

cesses in horizontal and vertical space. Furthermore, the snowpack is represented as a single layer and is not discretized into multiple layers, a simplification of many natural snow covers. Nevertheless, since average snow grain sizes tend to increase during the course of the winter season, it is suggested that such a growth system could reflect the general behavior of a pack evolution.

Determination of the growth regime is achieved in different ways. Fresh snow undergoes negligible radius growth [24] and is assumed to last for four days, after which the other growth regimes take over as the sintering or faceting processes dominate growth. Whether or not kinetic or equitemperature growth regimes are prominent depends on the thermal gradient through the snowpack. Under a large thermal gradient (greater than $10 \text{ }^{\circ}\text{C m}^{-1}$) that persists for ten days or more [32], kinetic growth is assumed to dominate and (2) is applied. Estimation of the thermal gradient is problematic since the snow depth is not known *a priori*. Therefore, an alternative metric is used as an index of thermal gradient. We estimate the difference between surface physical temperature and snow/soil interface temperature as a gradient temperature indicator. It is assumed that the underlying surface soil temperature is $0 \text{ }^{\circ}\text{C}$. To estimate the surface air temperature of a snowpack, a multiple linear regression using the least squares criterion was obtained between surface air temperature (T), recorded in the four-year WMO-GTS data, and coincident SSM/I channel brightness temperatures such that

$$T = 58.08 - 0.39T_{b19V} + 1.21T_{b22V} - 0.37T_{b37H} + 0.36T_{b85V} \text{ [K]}. \quad (3)$$

The standard error of the regression is 6.9 K, and the coefficient of determination is 0.8. It is assumed that under low cloud liquid water conditions, typically observed in winter and at high elevations or northern latitudes (most snow is found north of 40° N latitude), the emissivity is high enabling reasonable estimation of surface temperatures. Improved estimates of surface temperature will be obtained from mesoscale climate models as the algorithm is updated.

Fig. 2 shows time series of the temperature difference between snowpack surface and base and of grain size evolution for a meteorological station in Russia. The grain radius gradually

increases through the season with the rate of change controlled by the growth regime in turn a function of temperature difference through the pack. The characteristics of the curve reflect general observations of grain growth with a gradually increasing average radius through the season. However, the model is not equipped to simulate localized, complex short-term changes in the pack that are found in many parts of the world; this ability for the model would require detailed knowledge of a snowpack's energy budget, which is not available in remote regions. Nevertheless, the model does provide an indication of how the grid-cell averaged grain size might change through time. Validation of this curve without ground observations is difficult if not impossible unless a dedicated field experiment were set up. The Cold Land Processes Field Experiment, supported by NASA's Land Surface Hydrology Program, currently underway will assist in quantifying changes in grain size from mid season to melt season at a spatially intensive set of field sites in Colorado [33].

C. Densification Model

The microwave emission from a snowpack is directly affected by bulk snow density [27]. To determine its effect through the season, a dynamic representation of snow density is required that can encapsulate the general seasonal trend of snow density variation. Generally, it is known that snow density increases from the time when the snow is fresh to when it is a mature snowpack [34]. Fresh snow density is often less than 100 kg m^{-3} (e.g., [35]), while mature snow densities can range from $200\text{--}400 \text{ kg m}^{-3}$ (e.g., [36]) depending on the complex metamorphic processes operating locally. In an effort to keep the estimation of density straightforward, we implement a simple logistic curve of seasonal snow density growth that is very similar to the grain growth curve in (2)

$$mv(t) = mv_{s\infty} - (mv_{s\infty} - mv_{s0}) \exp(-lt) \text{ [mm]} \quad (4)$$

where $mv_s(t)$ is the snow volume fraction (%) at time t in days, mv_{s0} is the fresh snow volume fraction (%) at deposition, $mv_{s\infty}$ is the maximum snow volume fraction (%) and l is the densification rate which we set to 0.007. This value produces a slowly increasing volume fraction through the season. Volume fraction is related to density simply by dividing the density by 900 kg m^{-3} such that 0% volume fraction equates to 0 kg m^{-3} and 100% volume fraction equals 900 kg m^{-3} . The initial snow volume fraction is obtained from the expression of [37]

$$mv_{s0} = [67.92 + 51.25 \exp^{(T/2.59)}] / 900.0\% \quad (5)$$

where T is obtained from (3) and converted to degrees Celsius. [34] suggest that under several conditions, especially in the presence of strong wind, the density can rapidly increase within the first few hours. We therefore assume that an initial fast densification occurs of 50 kg m^{-3} (volume fraction 0.055%), and this is added to the initial fresh snow density. The maximum density is set to the sum of the fresh snow density plus 250 kg m^{-3} (volume fraction of 0.27%). Thus, the density increases through the season in a gentle exponential fashion. This model is a gross simplification of reality and in many cases will underestimate and overestimate snow density compared with reality. However, it provides a means of estimating a general "average"

snow density and how it changes through the season based on well-documented general properties of snow.

D. Coupling Grain Size Evolution and Densification Models to the DMRT Model

A full description of the DMRT model is presented in [38]. For the purpose of this work and in keeping with the theoretical assumptions in the model, the estimates of brightness temperatures are used from moderate grain radii of between 0.2 and 1.0 mm. For simplicity, it is assumed that the snow temperature is constant at 260 K. In fact the DMRT simulation data does show that temperature has an effect on the snow depth estimate. The effect is small at large grain sizes; at 0.5 mm, the difference in snow depth for a 250-K pack and a 270-K pack is 2 cm. At small grain sizes (0.3 mm) the difference in snow depth between a 250-K and 270-K snowpack is 12 cm. By setting the temperature to 260 K the errors of temperature should be restricted to less than 7 cm. While this is a simplification of our understanding of snowpack conditions, its importance is considered to be of secondary nature compared with the density and grain radius in controlling the microwave emission response.

We use the brightness temperature differences between the Tb19V and Tb37V (henceforth referred to as ΔTb) to estimate the snow depth under the assumed snow temperature constraint. Fig. 3 shows the corresponding set of curves relating ΔTb to snow depth for the range of snow grain radii between 0.2 and 0.6 mm. The curves show gradually decreasing gradients as the snow grain radius increases for each volume fraction. Theoretically, this is expected since larger grains tend to scatter microwave radiation more than smaller grains. The solid curved lines are polynomials fitted using linear least square criterion for each radius simulation. These relationships are calculated only for the linear portion of the DMRT from [38]; the DMRT model predicts saturation of the ΔTb at large grain sizes. This aspect is addressed later.

It was necessary to couple the grain radius and volume fraction data with the DMRT model data. In Fig. 3, the curves have a coefficient of determination of at least 0.98 which gives confidence to these polynomials. The general form of the equations is

$$\text{SD} = b(\Delta\text{Tb})^2 + c(\Delta\text{Tb}) \text{ [cm]} \quad (6)$$

where b and c are coefficients empirically related to the grain size and the volume fraction thus

$$b = 0.898(\text{gs}/\text{mv})^{-3.716} \quad (7a)$$

$$c = 1.060(\text{gs}/\text{mv})^{-1.915}. \quad (7b)$$

For (7a) the R^2 fit is 0.98, and for (7b) the R^2 is 0.83 lending reasonable confidence to this calibration. Hence, for any grain size and volume fraction predicted by the models, the parameters b and c in (6) can be estimated using (7a) and (7b). Then, using the SSM/I data at Tb19V and Tb37V, a unique snow depth can be estimated from the predicted DMRT model equation.

One problem that arises with the application of the ΔTb is that it is known that at 37 GHz, the Tb will saturate at snow depths of approximately 100 times the wavelength. This can occur at between 50 and 100 cm of snow depth depending on

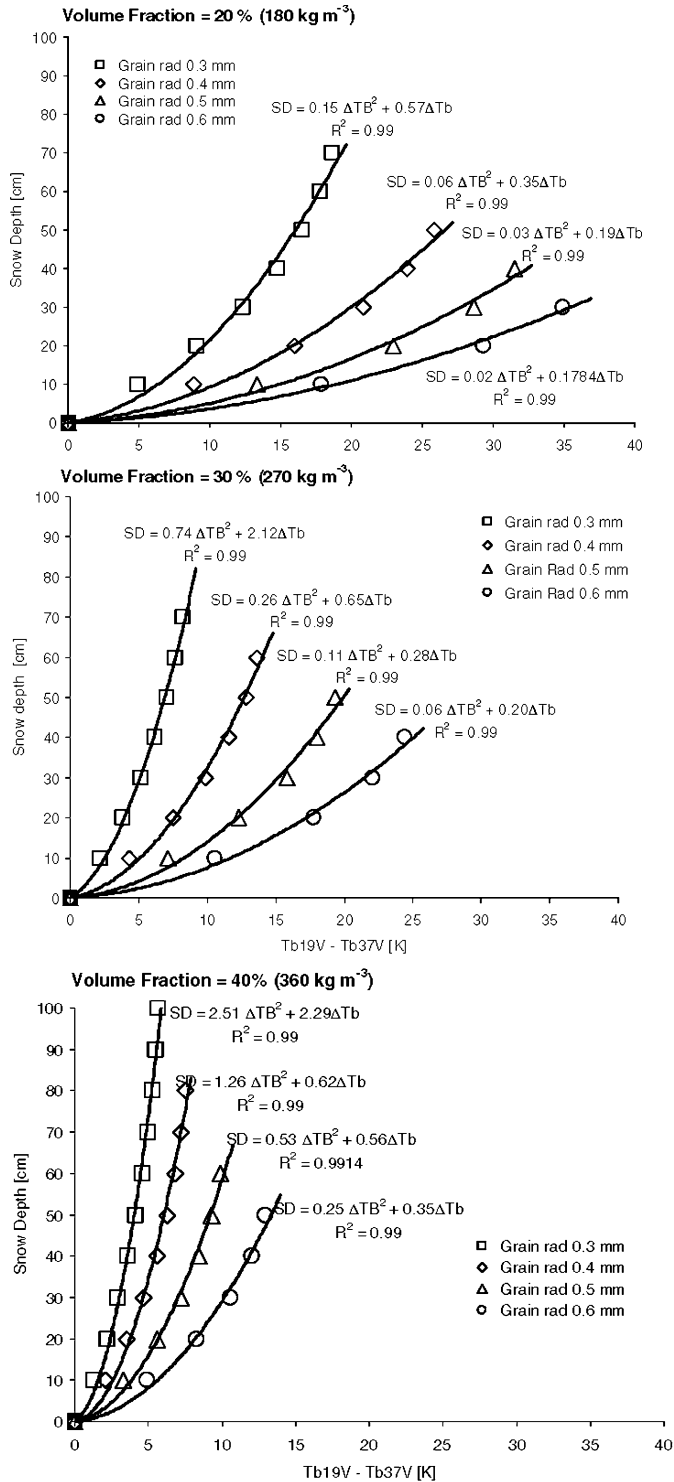


Fig. 3. Inverted DMRT relationships between brightness temperature differences ($T_{b19V} - T_{b37V}$) and snow depth for three volume fractions of 20%, 30%, and 40%. The curves represent the relationships for a range of moderately sized snow grains. The R^2 values refer to the polynomial fits calculated using the least squares criterion.

the grain size and volume fraction components (as illustrated in Fig. 2). Hence, we set limits for this threshold based on the following linear regression relation derived from the DMRT simulation in Fig. 3:

$$\text{satK} = 15.09(\text{gs/mv}) - 5.79 [\text{K}]. \quad (8)$$

The saturation temperature of ΔT_b for a given grain size and volume fraction is represented as satK . Again the R^2 is high at 0.96 lending confidence to this parameterization. The check ensures that the brightness temperatures from the instrument are used only within the range of the calibration of the DMRT model; if ΔT_b is greater than satK then satK is substituted for the ΔT_b in (6).

The approach developed here is a simplified estimation of DMRT model ΔT_b -snow depth curves. Rather than matching DMRT model estimated brightness temperature profiles with SSM/I brightness temperatures for a well-constrained set of snowpack parameters (as described in [38]), we use the DMRT model in a deterministic way. Clearly, generalizations about the snowpack condition and its evolution are made which at an instance or location may or may not be valid. It also uses one realization of the DMRT model based on specific assumptions. However, this empirical approach precludes the need for detailed local meteorological data to drive a snow model and can be applied in a wide geographical context.

E. Inclusion of Snowpack History in Snow Depth Estimation

The methodology described earlier is implemented to provide an “instantaneous” daily snow depth estimate. However, it is evident that in many instances, passive microwave brightness temperatures can vary as the average snowpack physical conditions within a footprint vary. For example, melt/refreeze events can alter the brightness temperature profile over a short time; the scattering may become reduced, or it may be enhanced by these events depending on the spatial extent. Fig. 4 shows the time series of ΔT_b for the station in Russia. The short-term, high-magnitude fluctuations are especially prominent at the end of the winter seasons when the pack undergoes strong melt/refreeze processes. Since the grain growth model does not account for such events, it is necessary to use the immediate history of the snow depth estimates to smooth the instantaneous estimates. This implies that an estimate of snow depth is related to its recent history; an assumption that is not dissimilar to conditions found in natural snowpacks. Fig. 4 also shows the ten-day running standard deviation of the estimated snow depth immediately preceding the estimate. The spikes in these data are especially evident at the end of the season when the pack is undergoing rapid thermal changes. To overcome this problem a five-day Gaussian weighted mean filter was applied as described by Holloway [39]. If the standard deviation for the five days is large, then the filtered mean is weighted more evenly over the five days. If the standard deviation is small, then the mean is weighted more from most recent estimates. This filter has an advantage over a simple running mean in that it retains better the phase of the time series. Fig. 5 shows the smoothed estimated snow depth for the 1992–1995 dataset for the Russian station. The instantaneous data are also plotted on the curve so that the effect of this filter can be seen. The smoothed snow depth data show a reduction of the high frequency fluctuations that are more related to changes in the snowpack physical conditions rather than variations in snow depth.

In summary, the algorithm is a combination of an empirical grain radius growth model and a densification model that are used to parameterize a constrained DMRT model suite of

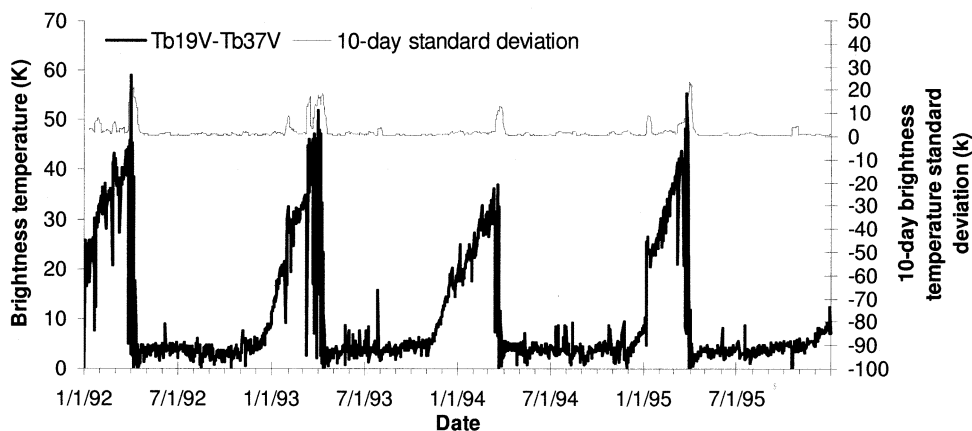


Fig. 4. Variation of the scattering index (Tb19V-Tb37V) and ten-day standard deviation of the scattering index during the 1992–1995 period for the station in Russia (58° 52′ 12″ N, 78° 21′ 00″ E).

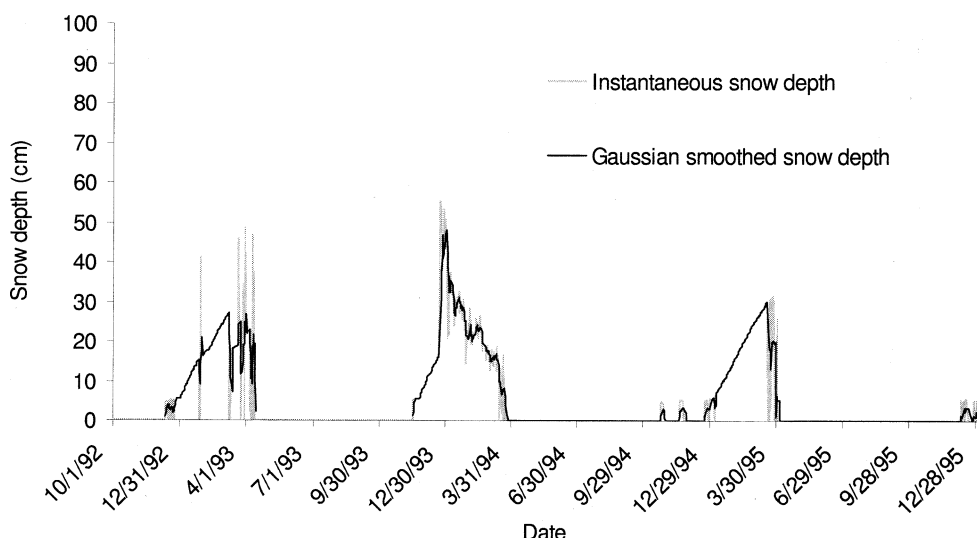


Fig. 5. Time series of instantaneous snow depth estimates and smoothed snow depth estimates from the dynamic algorithm for the Russian station located at 58° 52′ 12″ N, 78° 21′ 00″ E.

snow depth estimates from brightness temperature differences observed by the passive microwave instrument (in this case the SSM/I). Instantaneous values are then smoothed based on the preceding snow depth history. Fig. 6 shows an example of the algorithm applied to the 2000–2001 data with three final smoothed estimates of global snow cover at the start, middle and end of the snow season. Consistency is found especially at high latitudes where the snowpack tends to be the most stable.

V. TESTING THE ALGORITHM

The dynamic algorithm was applied to data at each station in the 1992–1995 WMO-GTS period and for the 2000–2001 period, which had 90 snow days between December and April (inclusive) that were used for validation in order to ensure that temporally coherent snowpacks were tested. Estimated snow depth values were compared with observations made on the ground at each station and only ground measured snow depths greater than 3 cm were used in the comparison because microwave response to thinner snowpacks at 37 GHz is negligible. The comparison was on a pixelwise basis and an assumption was made

that each SSM/I estimate at 25×25 km was equivalent in scale to the point observation of snow depth on the ground. In addition to the dynamic algorithm developed here, the algorithm described in [13] was implemented and both passive microwave methods were compared to determine whether an improvement using the dynamic grain growth algorithm could be detected. For the 1992–1995 period, only complete winter season datasets were used (i.e., data comprising the 1992/1993, 1993/1994, and 1994/1995 seasons), since for the incomplete seasons, the dynamic model could not be initialized adequately. A subtle difference between SSM/I data used in these two datasets is also noted. For the 1992–1995 data, the SSM/I data were averaged around each meteorological station location such that the SSM/I channel values used were the result of a 3×3 pixel average. This was done in the initial data preparation stages prior to the data being released, and we had no control over the process. In fact, it is expected that the smoothing process might enhance the scattering signal (ΔT_b) by lowering the mean T_b at 37 GHz relative to 19 GHz on account of the greater spatial resolution at the 37 GHz. The smoothing was not performed for the 2000–2001 dataset.

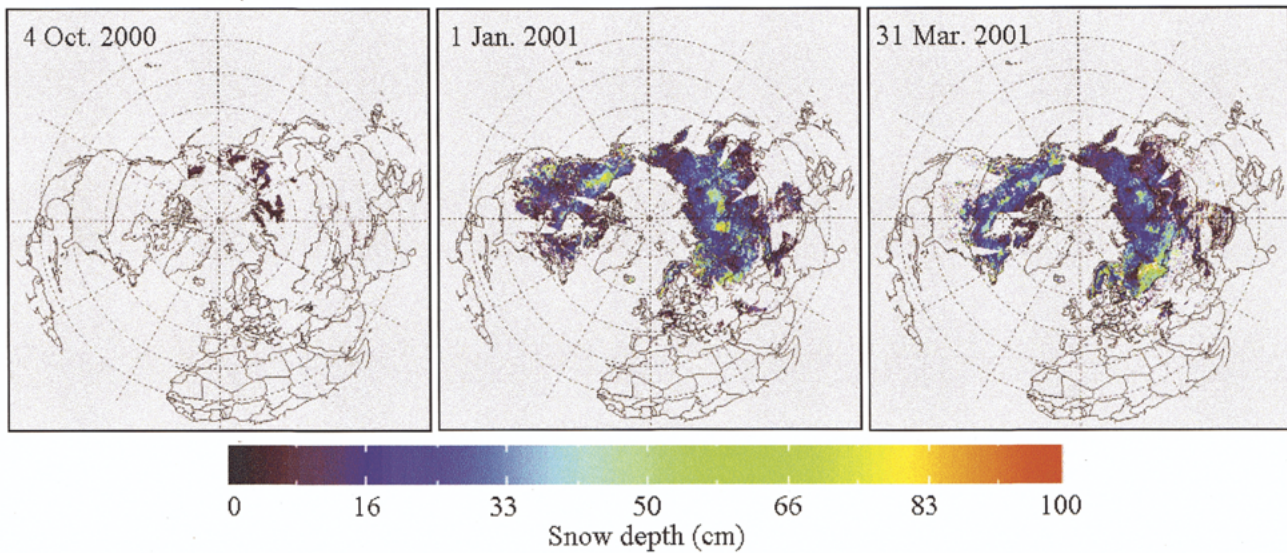


Fig. 6. Example of the dynamic snow depth estimation algorithm for start middle and end of the 2000–2001 winter season.

TABLE II
GLOBAL MEAN SNOW DEPTH (SD) ERROR STATISTICS FROM THE IMPLEMENTATION OF THE STATIC AND DYNAMIC ALGORITHMS TO THE 1992–1995 NORTHERN HEMISPHERE STATION DATA

Metric	Standard errors (cm)			Total Mean Relative Errors (%)				Max. SD	Mean max. SD
	RMSE	ME	MAE	Ave.	Mode	Median	St. Dev.		
Static	14.5	-5.9	9.8	79.1	61.0	58.5	37.5	137.0	40.7
Dynamic	20.5	-5.7	17.6	94.0	44.0	66.2	92.3	137.0	40.7

TABLE III
GLOBAL MEAN SNOW DEPTH (SD) ERROR STATISTICS FROM THE IMPLEMENTATION OF THE STATIC AND DYNAMIC ALGORITHMS TO THE 2000–2001 NORTHERN HEMISPHERE STATION DATA

Metric	Standard errors (cm)			Total Mean Relative Errors (%)				Max. SD	Mean max. SD
	RMSE	ME	MAE	Ave.	Mode	Median	St. Dev.		
Static	18.5	-10.5	16.3	77.0	60.7	65.6	60.5	160.0	49.2
Dynamic	23.1	-1.7	19.7	131.4	78.4	74.5	154.8	160.0	49.2

One key problem with the ground observations of snow depth was that of quality control. For the 1992–1995 period, each of the 100 station time series were scrutinized and for obvious errors and anomalies, thus reducing the number of stations to 71. For the 2000–2001 data, this was not practical, as there were sometimes more than 1000 stations available for use. Thus, for this dataset, the snow depth data were smoothed automatically from the surrounding values using a sigma filter. If the gauge estimate was greater than one standard deviation from the mean of the surrounding four snow depth measurements, then the average of the four was used and the original value was discarded; otherwise the original value was used. In addition, only gauge data that were located away from large water bodies (e.g., oceans and lakes) and mountainous terrain were used in the verification stage. For the former surface type, the emissivity effect of water in a mixed land/water pixel often produces anomalous responses. In the case of mountainous terrain, complex brightness temperature responses are often observed on account of the snow being observed at multiple viewing angles.

Tables II and III give the results for the error statistics. The metrics used in the comparison between estimated and measured snow depth were the root-mean-squared error (RMSE) (sometimes termed the standard error), the mean absolute error (MAE), and the mean error (ME). RMSE, ME, and MAE were computed for each station for the 1992–1995 time series and for each station for the 2000–2001 series. Also, for each season, mean relative error statistics were calculated for each station. This metric is the difference between measured and estimated snow depth expressed as a percentage of the measured snow depth. Then, the global seasonal average, median, mode, and standard deviation of station mean relative errors was calculated.

The dynamic retrieval algorithm developed in this paper shows no improvement in RMSE over the static algorithm for the 1992–1995 dataset. However, the ME is slightly closer to zero than the static ME, although the MAE is worse than the static algorithm (17.6 and 9.8 cm, respectively). These results are disappointing with little or no improvement overall in

the dynamic algorithm apparent from these metrics. However, inspection of the mean relative error statistics shows that there is a definite skew in the performance of the dynamic algorithm as represented by the station statistics. The mean global seasonal average relative error of the dynamic algorithm is 94.0%, while the mode is 44.0% and the median 66.2%. There is clearly a skew in the data, suggesting that a few stations are exerting a strong bias on the global seasonal means. This is why the average relative errors are high and the standard deviations high (and the RMSE value is abnormally large). If comparisons are made between the mode and the median relative errors, there is better agreement between the static and dynamic algorithms. To indicate the range of snow depths, for which these errors are found, the last two columns in Table II give the absolute maximum station snow depth and the average station maximum snow depth. The minimum snow depth is 3 cm.

Fig. 7 shows a plot of the variation in global seasonal average per station RMSE in the 1992–1995 dataset. Both algorithm RMSE values are plotted as a function of mean seasonal snow depth measured at each station. For best results, one would expect the RMSE values to remain low over the full range of snow depths. However, in both cases, the RMSE increases with increased snow depth. One possible reason for this increase in error with increased snow depth is that the microwave response saturates generally at snow depths greater between 50 and 100 cm (depending on density and grain size). Since the DMRT model implementation is calibrated to account for saturation, if the measured snow depth is greater than the saturation threshold, errors will result. Therefore, further development of the dynamic algorithm should focus on scattering signals at lower frequencies that do not saturate until the snow is thicker. Another possibility for the trend in Fig. 7 is that the gauge snow depth data are not spatially representative of the SSM/I footprint, especially when the snow depth is large. Local-scale snow spatial variability studies at the passive microwave footprint scale will help to clarify this issue.

Fig. 8 shows an example of two snow maps for the February 10, 2001 in the Northern Hemisphere using the static and dynamic algorithms. Microwave data observed before 14:00 local time were used, which explains the improved coverage at higher latitudes and the reduced coverage at lower latitudes. The spatial distributions of snow depth are similar except that the dynamic algorithm estimates shallower snowpacks in general around the Northern Hemisphere. Table III shows the error statistics from the comparison between estimated and measured snow depth for the 2000–2001 winter season. For this case study, the RMSE values are greater for both algorithms than for the 1992–1995 dataset. There are many more stations used in this analysis and on some days over 1000 gauges recordings taken. While the RMSE for the dynamic algorithm again is greater than the static algorithm, the ME of the dynamic algorithm is 8.8 cm better than the ME of the static algorithm. It is interesting to note that the global average seasonal snow depth measured at all WMO-GTS stations used in the comparison is 25.5 cm, while the average estimated global snow depth from the static algorithm is 14.4 cm. The global average seasonal snow depth for the dynamic algorithm is 24.4 cm, which is remarkably close to

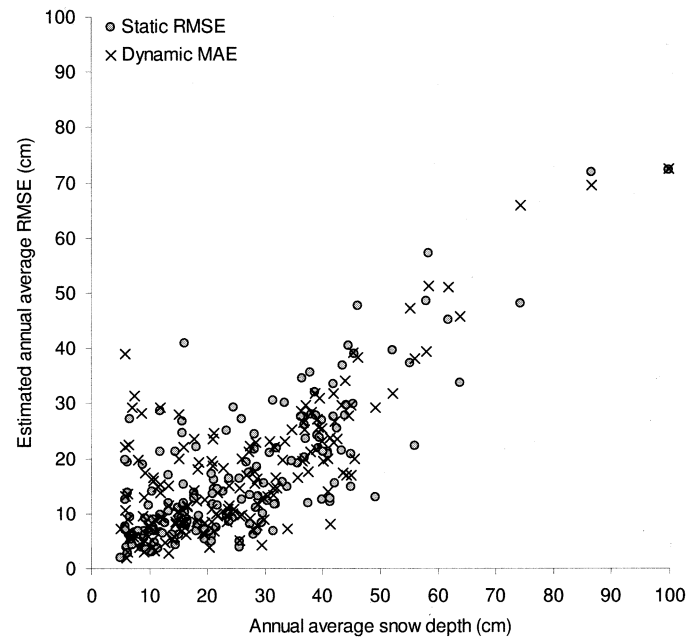


Fig. 7. Variation in RMSE for static and dynamic snow depth algorithms as a function of mean station snow depth over the three-year period.

the measured seasonal average. It is also noteworthy that compared with the static algorithm ME, the dynamic algorithm ME is closer to 0 cm by over 8.8 cm; the dynamic algorithm on average tends to underestimate the snow depth less than the static algorithm. This seems to be a significant improvement. Again, there are several locations in the comparison that are significantly biasing the results for the dynamic model as shown by the average, mode and median total mean relative error statistics. Further analysis of these locations is required and data from other winters are being examined to determine the variability of these outcomes.

In an effort to determine whether any geographical biases in the data are present, Fig. 9 shows the average seasonal ME values for the Northern Hemisphere for both algorithms. The contour lines are lines of equal ME with the red isolines representing snow depth overestimation and the light and dark blue isolines representing underestimation. Yellow represents mean errors close to zero (or little bias). The underestimation of the static model is evident especially in the Eurasian boreal forest areas with a large swath of light to midblue isolines extending from eastern Europe to Siberia. To the south of this area, the algorithm does reasonably well with an average zero ME (yellow isoline). In northeast Asia, the algorithm tends to underestimate the snow depth by between 0 and 30 cm, and in northeast Canada there is significant snow depth underestimation. The dynamic model, however, does not underestimate snow depth over such a large area as the static model especially in central Siberia and northeast Canada. In addition, it tends to overestimate snow depth in the marginal southern areas by between 10 and 30 cm. In central-north and northeast Asia the dynamic model underestimates the snow depth but by less than the static model. This is probably caused by the lack of account made by the dynamic model of forest cover, which is known to affect passive microwave radiation. These results

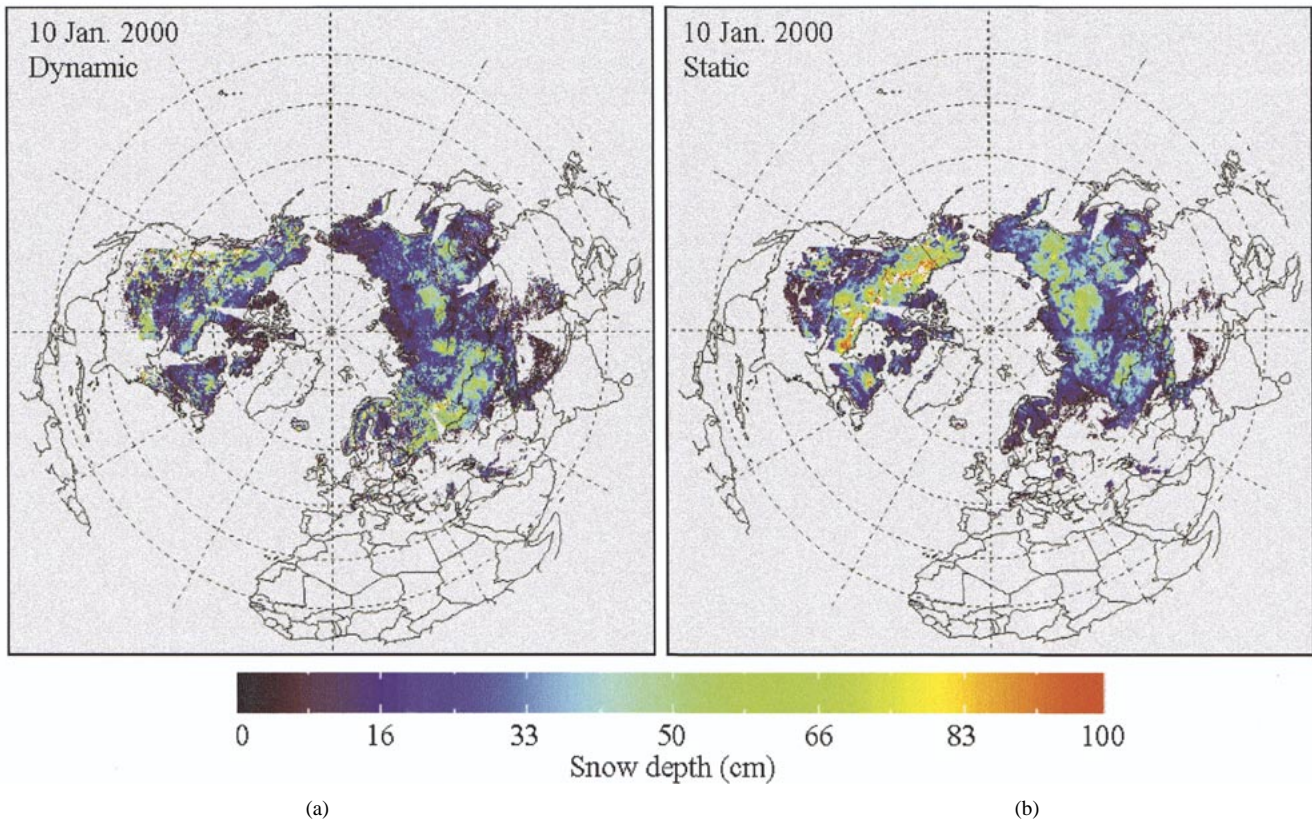


Fig. 8. Comparison of snow depth for 10 January 2001 estimated using the static and dynamic algorithms.

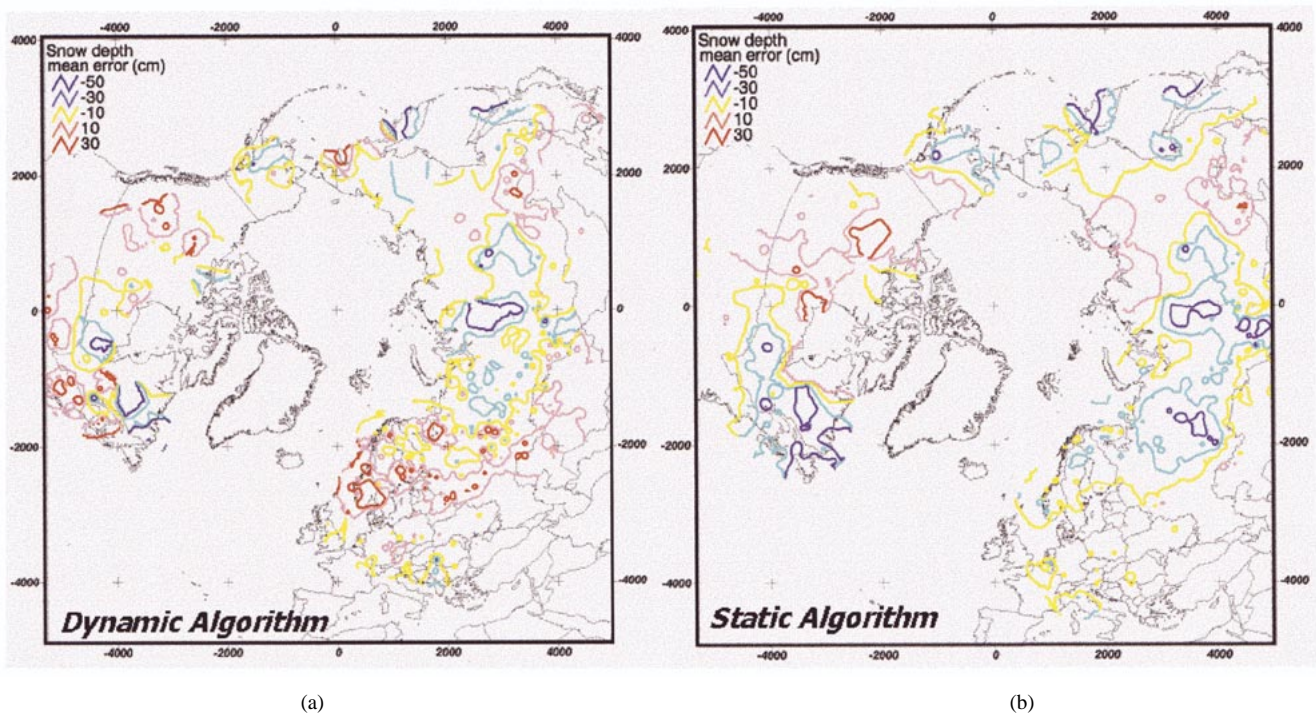


Fig. 9. Contour maps of the average seasonal errors for 2000-2001 winter season for the static and dynamic snow depth algorithms. Contour lines represent lines of equal over- or underestimation of snow depth.

give some spatiality to the statistics in Table III. However, they point to the need for improvement to the model dynamics and a need to incorporate information about vegetation cover, especially forests.

VI. CONCLUSION

A dynamic approach to retrieve global snow depth estimation is presented. Compared with static approaches developed in the

past, the dynamic algorithm tends to estimate snow depth with greater RMSE values but lower ME values (bias). These results are promising, but there is a need for further improvement and refinement to the algorithm especially in terms of identifying and reducing the elements of the models that contribute to large errors. The dynamic model builds on original work by Chang *et al.* [5], Foster *et al.* [13], and Tsang *et al.* [38]. In essence, it adjusts the coefficient in (1) by predicting how the grain size might vary and how this affects the emission from a snowpack. In addition, by incorporating a time smoothing function, the estimates are made temporally dependant. The algorithm can still be improved, however. Refinement is needed to the grain size and volume fraction evolution models since its empirical functions are space independent; Sturm and Holmgren [40] have shown that a seasonal snow cover classification is possible based on dominant geographically varying snow climatology. This information could be used further to improve the parameterization of (2). In addition, the planned Moderate Resolution Imaging Spectroradiometer (MODIS) snow albedo product could potentially be of great help with the grain size evolution. A snowpack's surface grain size can be related to its albedo and this information could be very useful especially at the start of the season when snow grain sizes are critical for the model. Also, the density model is very simple and needs further refinement to account for variable changes to snow density. This is more problematic, but could be addressed using a multisensor approach to determine more accurately the snow surface thermal environment.

With the availability of AMSR-E data, some of the snow depth retrieval problems should be reduced. For example, with AMSR-E's improved spatial resolution, snow detection capabilities ought to improve especially for the identification of shallow snowpacks at the start of the season. Although these early season packs are not as hydrologically significant as the midseason packs, they can influence the evolutionary characteristics of the snow, which are important for microwave retrievals. In addition, with AMSR-E's expanded range of channels at lower frequencies, characterization of the subnivean snow surface should improve, and it is possible that there will be potential for greater quantification of selected internal snowpack properties of pack (especially liquid water content). Finally, the potential for combining snow maps from MODIS with snow depth and SWE retrievals from AMSR-E will make a powerful tool for climate studies and global water resource management.

ACKNOWLEDGMENT

The authors would like to thank the National Space Development Agency of Japan/Earth Observation Research Centre for providing SSM/I and snow depth data used in this paper. The authors would also like to thank the referees for helpful comments.

REFERENCES

- [1] J. Cohen and D. Entekhabi, "Eurasian snow cover variability and Northern Hemisphere climate predictability," *Geophys. Res. Lett.*, vol. 26, pp. 345–348, 1999.
- [2] A. Frei and D. A. Robinson, "Northern Hemisphere snow extent: Regional variability 1972–1994," *Int. J. Climatol.*, vol. 19, pp. 1535–1560, 1999.

- [3] D. K. Hall, R. E. J. Kelly, G. A. Riggs, A. T. C. Chang, and J. L. Foster, "Assessment of the relative accuracy of hemispheric-scale snow-cover maps," *Ann. Glaciol.*, vol. 34, pp. 24–30, 2002.
- [4] D. K. Hall, J. L. Foster, V. V. Salomonson, A. G. Klein, and J. Y. L. Chien, "Development of a technique to assess snow-cover mapping errors from space," *IEEE Trans. Geosci. Remote Sensing*, vol. 39, pp. 432–438, Feb. 2001.
- [5] A. T. C. Chang, J. L. Foster, and D. K. Hall, "Nimbus-7 derived global snow cover parameters," *Ann. Glaciol.*, vol. 9, pp. 39–44, 1987.
- [6] C. Chen, B. Nijssen, J. Guo, L. Tsang, A. W. Wood, J. Hwang, and D. P. Lettenmaier, "Passive microwave remote sensing of snow constrained by hydrological simulations," *IEEE Trans. Geosci. Remote Sensing*, vol. 39, pp. 1744–1756, Aug. 2001.
- [7] R. L. Armstrong and M. J. Brodzik, "Recent Northern Hemisphere snow extent: A comparison of data derived from visible and microwave satellite sensors," *Geophys. Res. Lett.*, vol. 28, pp. 3673–3676, 2001.
- [8] J. Pulliainen and M. Hallikainen, "Retrieval of regional snow water equivalent from space-borne passive microwave observations," *Remote Sens. Environ.*, vol. 75, pp. 76–85, 2001.
- [9] A. T. C. Chang *et al.*, "Algorithm theoretical basis document (ATBD) for the AMSR-E snow water equivalent algorithm," NASA/GSFC, Greenbelt, MD, Nov. 2000.
- [10] J. P. Hollinger, J. L. Pierce, and G. A. Poe, "SSM/I instrument evaluation," *IEEE Trans. Geosci. Remote Sensing*, vol. 28, pp. 781–790, Sept. 1990.
- [11] B. Goodison and A. Walker, "Canadian development and use of snow cover information from passive microwave satellite data," in *Passive Microwave Remote Sensing of Land-Atmosphere Interactions*, B. Choudhury, Y. Kerr, E. Njoku, and P. Pampaloni, Eds. Utrecht, Netherlands: VSP BV, 1994, pp. 245–62.
- [12] A. T. C. Chang, J. L. Foster, D. K. Hall, A. Rango, and B. K. Hartline, "Snow water equivalent estimation by microwave radiometry," *Cold Reg. Sci. Technol.*, vol. 5, pp. 259–267, 1982.
- [13] J. L. Foster, A. T. C. Chang, and D. K. Hall, "Comparison of snow mass estimates from a prototype passive microwave snow algorithm, a revised algorithm and snow depth climatology," *Remote Sens. Environ.*, vol. 62, pp. 132–142, 1997.
- [14] M. T. Hallikainen and P. Jolma, "Comparison of algorithms for retrieval of snow water equivalent from Nimbus-7 SMMR data in Finland," *IEEE Trans. Geosci. Remote Sensing*, vol. 30, pp. 124–131, Jan. 1992.
- [15] R. L. Armstrong, A. T. C. Chang, A. Rango, and E. Josberger, "Snow depths and grain-size relationships with relevance for passive microwave studies," *Ann. Glaciol.*, vol. 17, pp. 171–176, 1993.
- [16] F. T. Ulaby and W. H. Stiles, "The active and passive microwave response to snow parameters 2. water equivalent of dry snow," *J. Geophys. Res.*, vol. 85(C2), pp. 1045–1049, 1980.
- [17] P. Hoekstra and A. Delaney, "Dielectric properties of soils at UHF and microwave frequencies," *J. Geophys. Res.*, vol. 79, pp. 1699–1708, 1974.
- [18] M. T. Hallikainen, F. T. Ulaby, M. C. Dobson, M. A. Elrayes, and L. K. Wu, "Microwave dielectric properties of wet soil. 1. Empirical models and experimental observations," *IEEE Trans. Geosci. Remote Sensing*, vol. GE-23, pp. 25–34, Jan. 1985.
- [19] T. J. Schmugge, "Microwave remote sensing of soil moisture," in *Applications of Remote Sensing in Agrometeorology*, F. Toselli, Ed. Dordrecht, The Netherlands: Kluwer Academic, 1988, pp. 257–284.
- [20] A. T. C. Chang and T. Koike, "Progress in AMSR snow algorithm development," in *Microwave Radiometry and Remote Sensing of the Earth's Surface and Atmosphere*, P. Pampaloni and S. Paloscia, Eds. Utrecht, The Netherlands: VSP BV, 2000, pp. 515–523.
- [21] R. L. Armstrong and M. J. Brodzik, "An earth-gridded SSM/I data set for cryospheric studies and global change monitoring," *Adv. Space Res.*, vol. 10, pp. 155–163, 1995.
- [22] D. Yang and M.-K. Woo, "Representativeness of local snow data for large scale hydrologic investigations," *Hydrol. Process.*, vol. 13, pp. 1977–1988, 1999.
- [23] K. F. Dewey and R. Heim, Jr., "Satellite observations of variation in Northern Hemisphere seasonal snow cover," NOAA, NOAA Tech. Rep. NESS 87, 1981.
- [24] ———, "Satellite observations of variations in Southern Hemisphere snow cover," NOAA, NOAA Tech. Rep. NESDIS 1, 1983.
- [25] N. C. Grody and A. N. Basist, "Global identification of snowcover using SSM/I measurements," *IEEE Trans. Geosci. Remote Sensing*, vol. 34, pp. 237–249, Jan. 1996.

- [26] A. E. Walker and B. E. Goodison, "Discrimination of a wet snow cover using passive microwave satellite data," *Ann. Glaciol.*, vol. 17, pp. 307–311, 1993.
- [27] C. Mätzler, "Passive microwave signatures of landscapes in winter," *Meteorol. Atmos. Phys.*, vol. 54, pp. 241–260, 1994.
- [28] A. Rango, A. T. C. Chang, and J. L. Foster, "The utilization of spaceborne microwave radiometers for monitoring snowpack properties," *Nord. Hydrol.*, vol. 10, pp. 25–40, 1979.
- [29] S. Rosenfeld and N. C. Grody, "Metamorphic signatures of snow revealed in SSM/I measurements," *IEEE Trans. Geosci. Remote Sensing*, vol. 38, pp. 53–63, Jan. 2000.
- [30] S. C. Colbeck, "An overview of seasonal snow metamorphism," *Rev. Geophys. Space Phys.*, vol. 20, pp. 45–61, 1982.
- [31] M. Sturm and C. S. Benson, "Vapor transport, grain growth and depth hoar development in the sub-Arctic snow," *J. Glaciol.*, vol. 43, pp. 42–59, 1997.
- [32] A. Tait, "Estimation of snow water equivalent using passive microwave radiation data," *Remote Sens. Environ.*, vol. 64, pp. 286–291, 1998.
- [33] D. Cline, R. Armstrong, R. E. Davis, K. Elder, and G. Liston, "NASA cold land processes field experiment plan 2002–2004," in *NASA Earth Science Enterprise: Land Surface Hydrology Program*: NASA, 2001.
- [34] G. A. McKay and D. M. Gray, "The distribution of snowcover," in *Handbook of Snow: Principles, Processes, Management and Use*, D. M. Gray and D. H. Male, Eds. Toronto, ON, Canada: Pergamon, 1981, pp. 153–190.
- [35] A. Judson and N. Doeksen, "Density of freshly fallen snow in the Central Rocky Mountains," *Bull. Amer. Meteorol. Soc.*, vol. 81, pp. 1577–1587, 2000.
- [36] W. Wenshou, Q. Dahe, and L. Mingzhe, "Properties and structure of the seasonal snow cover in the continental regions of China," *Ann. Glaciol.*, vol. 32, pp. 93–96, 2001.
- [37] N. R. Hedstrom and J. W. Pomeroy, "Measurements and modeling of snow interception in the boreal forest," *Hydrol. Process.*, vol. 12, pp. 1611–1625, 1998.
- [38] L. Tsang, C. Chen, A. T. C. Chang, J. Guo, and K. Ding, "Dense media radiative transfer theory based on quasicrystalline approximation with applications to passive microwave remote sensing of snow," *Radio Sci.*, vol. 35, pp. 731–749, 2000.
- [39] J. L. Holloway, Jr., "Smoothing and filtering of time series and space fields," in *Advances in Geophysics*, H. E. Landsberg and J. Van Mieghem, Eds. New York: Academic, 1958, vol. 4, pp. 351–389.
- [40] M. Sturm, J. Holmgren, and G. E. Liston, "A seasonal snow cover classification system for local to global applications," *J. Climate*, vol. 8, pp. 1261–1283, 1995.



Richard E. Kelly received the B.S. degree from the University of Manchester, Manchester, U.K., in 1987, the M.A. degree from Wilfrid Laurier University, Waterloo, ON, Canada, in 1990, and the Ph.D. degree from Bristol University, Bristol, U.K., in 1995, all in geography.

From 1994 to 2002, he was a Lecturer of physical geography at the School of Geography, Birkbeck College, University of London, London, U.K., and in 2000, was invited to work at the Hydrological Sciences Branch, NASA Goddard Space Flight Center (GSFC), Greenbelt, MD. He is currently affiliated with NASA/GSFC as a Research Associate through Goddard Earth Science and Technology Center, University of Maryland—Baltimore County, Baltimore, MD. His research interests are in microwave remote sensing and spatial and hydrological modeling of the terrestrial cryosphere, especially snow and ice. He has participated in numerous snow and ice field experiments in the U.K., Switzerland, France, Norway, Pakistan, the Czech Republic, Canada, and the USA.

Alfred T. Chang (M'88–SM'91–F'01) received the B.S. degree in physics from National Cheng Kung University Tainan, Taiwan. He received the M.S. degree in 1970 and the Ph.D. degree in 1971, both in physics, from the University of Maryland, College Park.

He was an NAS/NRC Resident Research Associate at NASA Goddard Space Flight Center (GSFC), Greenbelt, MD, from 1972 to 1974, and joined NASA GSFC in 1974. His current position is Research Scientist with the Hydrological Sciences Branch, Laboratory for Hydrospheric Processes, NASA GSFC. His research expertise and experience include microwave remote sensing, microwave sensor systems, and radiative transfer modeling of the atmosphere, rain, snow, and soils. In 1993, he was appointed to be the Deputy Project Scientist for the Aqua (EOS-PM) project. He has authored and coauthored more than 100 refereed papers.

Dr. Chang was elected a Fellow of the Institute of Electrical and Electronics Engineers (IEEE) in 2001 for his contributions to the development of microwave remote sensing of rain and snow. He received the NASA Medal for Exceptional Scientific Achievement as a result of his microwave radiative transfer research in 1988. In 1996, he received the NASA GSFC Exceptional Achievement Award for the use of microwave remote sensing data to investigate hydrology from space. He is a member of the American Geophysical Union, American Meteorological Society, and URSI commission F.



Leung Tsang (S'73–M'75–SM'85–F'90) was born in Hong Kong. He received the S.B., S.M., and the Ph.D. degrees from the Massachusetts Institute of Technology, Cambridge.

He is currently a Professor of electrical engineering at the University of Washington, Seattle, where he has taught since 1983. Starting September 2001, he has been on leave from the University of Washington and is a Professor Chair and Assistant Head of the Department of Electronic Engineering, the City University of Hong Kong. He is a coauthor

of four books: *Theory of Microwave Remote Sensing* (New York: Wiley-Interscience, 1985), *Scattering of Electromagnetic Waves, Vol. 1: Theory and Applications* (New York: Wiley-Interscience, 2000), *Scattering of Electromagnetic Waves, Vol 2: Numerical Simulations* (New York: Wiley-Interscience, 2001), and *Scattering of Electromagnetic Waves, Vol 3: Advanced Topics* (New York: Wiley-Interscience, 2001). His current research interests include wave propagation in random media and rough surfaces, remote sensing, high-speed interconnects, computational electromagnetics, wireless communications, and optoelectronics.

Dr. Tsang was Editor-in-Chief of the IEEE TRANSACTIONS ON GEOSCIENCE AND REMOTE SENSING. He was the Technical Program Chairman of the 1994 IEEE Antennas and Propagation International Symposium and URSI Radio Science Meeting, the Technical Program Chairman of the 1995 Progress in Electromagnetics Research Symposium, and the General Chairman of the 1998 IEEE International Geoscience and Remote Sensing Symposium. He is a Fellow of the Optical Society of America and the recipient of the Outstanding Service Award of the IEEE Geoscience and Remote Sensing Society for 2000. He was also a recipient of the IEEE Third Millennium Medal in 2000. He is also an ADCOM member of the IEEE Geoscience and Remote Sensing Society.

James L. Foster received the B.S. and M.A. degrees in geography from the University of Maryland, College Park, and the Ph.D. degree in geography from the University of Reading, Reading, U.K., in 1995.

He has been with the Goddard Space Flight Center, Greenbelt, MD, as a member of the Hydrological Sciences Branch since 1978. His primary research interests involve remote sensing of snow (from various satellite and aircraft sensors) utilizing the visible and microwave portions of the electromagnetic spectrum. In addition, he has studied snow crystal structure and form using electron microscopy. His work is beneficial in helping to better manage water resources and in helping to better understand the possible impacts of changes in snow cover on climate. He has participated in research programs and field work that have taken him to Antarctica, Greenland, the Northwest Territories of Canada, Saskatchewan, Svalbard, and, in the United States, Alaska, the Rocky Mountains, the Great Plains, the Midwest, and New England.